

# 原子集団のCavity-QED (真空のラビ分裂を中心に)

2009.2.18 ランチミーティング

担当: 鳥井

## Cavity-QEDと言えば「単一原子観測」

C. J. Hood, *et. al.*, PRL **80**, 4157 (1998)

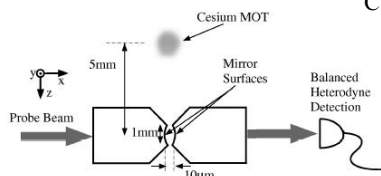
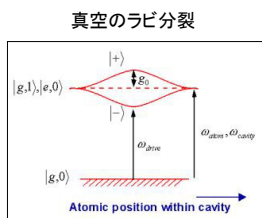
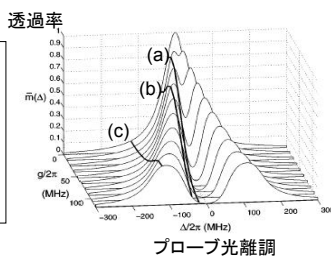


FIG. 1. Schematic of the experimental apparatus.

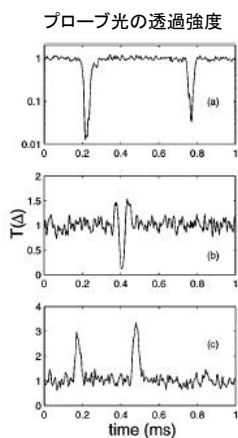


真空のラビ分裂



透過率

プローブ光離調



プローブ光の透過強度

# しかし2009.1.5にMin Xiaoがやってきて、こんな話をしていた

PRL 100, 173602 (2008)

PHYSICAL REVIEW LETTERS

week ending  
2 MAY 2008

## Observation of Intracavity Electromagnetically Induced Transparency and Polariton Resonances in a Doppler-Broadened Medium

Haibin Wu, J. Gea-Banacloche, and Min Xiao

Department of Physics, University of Arkansas, Fayetteville, Arkansas 72701, USA

(Received 24 September 2007; published 2 May 2008)

The transmission spectrum of three-level atoms in a vapor cell inside an optical cavity shows distinct peaks associated with atom-cavity polaritons in the system. We develop the theory of these resonances in a Doppler-broadened medium and present the results of experimental observations of these spectra in three-level  $\Lambda$ -type rubidium atoms inside an optical ring cavity.

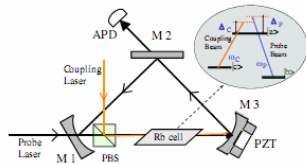


FIG. 1 (color online). Experimental setup. PBS, polarizing cubic beam splitters;  $M1$ – $M3$ , cavity mirrors; APD, avalanche photodiode detector; PZT, piezoelectric transducer.

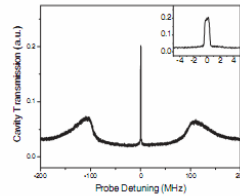


FIG. 2. The experimentally measured cavity transmission. The parameters are  $T = 67.7^\circ\text{C}$ ,  $\Omega = 120\text{ MHz}$ .

## こんなことを考えさせられた

- 真空のラビ分裂は電磁波の量子化(真空)が本質なのか(答えはNo)?
- 熱的原子(不均一幅を持つ媒質)で真空のラビ分裂が自然幅程度で見えるのは何故か?
- Cavity-QEDとEITを組み合わせると何が面白いのか?
- Cavity-QEDとBECを組み合わせると何が面白いのか?

### Vacuum-Field Rabi Splittings in Microwave Absorption by Rydberg Atoms in a Cavity

G. S. Agarwal

School of Physics, University of Hyderabad, Hyderabad-500 134, India  
(Received 20 June 1984)

The absorption spectrum of a system of  $N$  atoms interacting with a single mode of the quantized radiation field is exactly calculated. Such a spectrum shows vacuum-field Rabi splittings, and thus microwave absorption by Rydberg atoms in a cavity should be a useful way to observe these splittings.

$$H = \hbar \omega_0 \sum_i S_i^z + \hbar \omega a^\dagger a + \sum_i (\hbar g S_i^+ a + \text{H.c.}). \quad (1)$$

Here  $g$  is the coupling constant between the atom and the cavity mode which is represented by annihilation and creation operators  $a$  and  $a^\dagger$ . Each two-level atom is characterized by the spin- $\frac{1}{2}$  operators  $S_i^\pm$  and  $S_i^z$ . In terms of the collective variables  $\bar{S} = \sum_i S_i$ , (1) becomes

$$H = \hbar \omega_0 S^z + \hbar \omega a^\dagger a + (\hbar g S^+ a + \text{H.c.}). \quad (2)$$

This system is initially in the ground state  $|\psi_0\rangle$  with energy  $E_0$ :

$$|\psi_0\rangle = \left| \frac{N}{2}, -\frac{N}{2}; 0 \right\rangle, \quad E_0 = -\frac{N}{2} \hbar \omega_0. \quad (3)$$

Here  $|0\rangle$  represents the vacuum of the radiation field and  $|S, M\rangle$  represents the eigenstate of  $S^2$  and  $S^z$ . We will now calculate the quantum mechanical susceptibility of the system (1). Note that this is

be seen. Therefore we will work in the limit  $g\sqrt{N} \gg \kappa$ . The density matrix  $\rho$  for the combined atom-field system obeys

$$\frac{\partial \rho}{\partial t} = -\frac{i}{\hbar} [H, \rho] - \kappa (a^\dagger \rho a - 2a \rho a^\dagger + \rho a^\dagger a).$$

$g \rightarrow g\sqrt{N}$ . The absorption spectrum has a doublet structure with peaks at

$$\Omega = \omega_0 + \Delta/2 \pm \frac{1}{2} (\Delta^2 + 4Ng^2)^{1/2}, \quad (12)$$

with weight factors depending on  $\Delta$ ,  $g\sqrt{N}$ . For large detunings, the usual peak at  $\omega_0$  is recovered. For the resonant case  $\Delta=0$ , i.e., for the cavity mode on resonance with the atomic frequency, the peaks occur at

$$\Omega = \omega_0 \pm g\sqrt{N}, \quad (13)$$

### Normal-Mode Splitting and Linewidth Averaging for Two-State Atoms in an Optical Cavity

M. G. Raizen

Department of Physics, University of Texas at Austin, Austin, Texas 78712

R. J. Thompson, R. J. Brecha, H. J. Kimble, and H. J. Carmichael<sup>(a)</sup>

Norman Bridge Laboratory of Physics 12-33, California Institute of Technology, Pasadena, California 91125

(Received 3 April 1989)

An investigation of the radiative processes for a collection of  $N$  two-state atoms strongly coupled to the field of a high-finesse optical cavity is presented. Observations of the spectral response of the composite system to weak external modulation reveal a coupling-induced normal-mode splitting. Linewidth averaging leads to linewidths below the free-space atomic width.

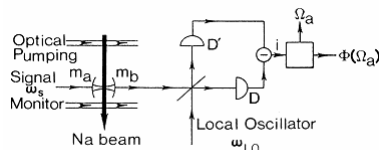


FIG. 1. Diagram of the apparatus as discussed in the text.

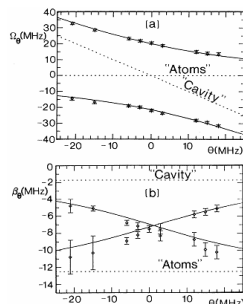
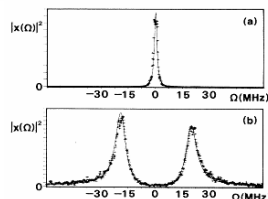


FIG. 4. Dependence of (a) normal-mode frequencies  $\Omega_a$  and (b) linewidths  $\Gamma_a$  on cavity detuning  $\Delta$  for fixed atomic detuning  $\Delta \approx 0$  in the weak-field limit. The data are obtained from traces similar to those in Fig. 2(b) with  $C=41$ ,  $\omega/\gamma=0.85$ . The full curves are the theoretical predictions for  $\Omega_a$  and  $\Gamma_a$  obtained from the Maxwell-Bloch equations with these parameters and  $\Gamma=0.8$ ; the dashed curves are for  $g=0$  (uncoupled atoms and cavity).

**Vacuum Rabi Splitting as a Feature of Linear-Dispersion Theory:  
Analysis and Experimental Observations**

Yifu Zhu, Daniel J. Gauthier, S. E. Morin, Qilin Wu, H. J. Carmichael, and T. W. Mossberg  
*Department of Physics and Chemical Physics Institute, University of Oregon, Eugene, Oregon 97403*  
 (Received 7 February 1990)

The spectral and temporal response of an optical cavity resonantly coupled to an ensemble of barium atoms has been investigated experimentally. The empty-cavity transmission resonances are found to split in the presence of the atoms and, under these conditions, the cavity's temporal response is found to be oscillatory. These effects may be viewed as a manifestation of a vacuum-field Rabi splitting, or as a simple consequence of the linear absorption and dispersion of the intracavity atoms.

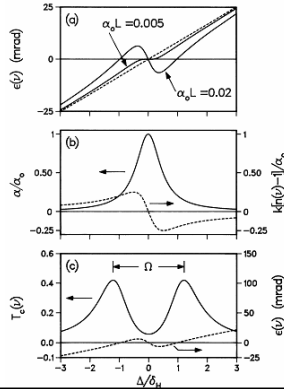


FIG. 1. (a) Phase shift experienced by the field upon completion of a round trip through the cavity for various values of the line-center, single-pass absorption as a function of the detuning of the probe-laser frequency from the atomic resonance frequency normalized to the atomic resonance width. The cavity resonance is tuned to the atomic resonance ( $\Delta_m = 0$ ),  $\Delta_{FSR}/\delta_H = 750$ ,  $\delta_c/\delta_H = 1.5$ , and  $F = 500$ . The dashed line is the empty-cavity phase shift. (b) Normalized absorption (solid line) and change in refractive index (dashed line) produced by the collection of Lorentz oscillators. The magnitude of the probe wave vector is denoted by  $k$ . (c) Cavity transmission function and phase shift as functions of the normalized frequency. The values of the parameters used to generate this plot are the same as in (a) with  $\alpha_0 L = 0.02$ .

**Observation of Normal-Mode Splitting for an Atom in an Optical Cavity**

R. J. Thompson, G. Rempe, and H. J. Kimble  
*Norman Bridge Laboratory of Physics 12-33, California Institute of Technology, Pasadena, California 91125*  
 (Received 4 November 1991)

An investigation of the spectral response of a small collection of two-state atoms strongly coupled to the field of a high-finesse optical resonator is described for mean number  $\bar{N} \leq 10$  atoms. For weak excitation, a coupling-induced normal-mode splitting is observed even for one intracavity atom, representing a direct spectroscopic measurement of the so-called vacuum Rabi splitting for the atom-cavity system.

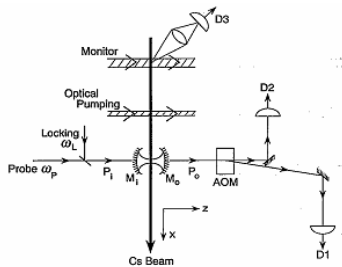


FIG. 1. Diagram of principal elements of the experiment.

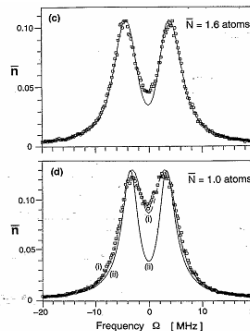


FIG. 2. Intracavity photon number  $\bar{n}$  vs probe frequency  $\Omega$  for four values of  $\bar{N}$  and with  $\alpha_0 L = \alpha_0$ . Curves in (a)-(c) and curve *i* in (d) are theoretical fits to the data including fluctuations in atomic number and position. Curve *ii* in (d) is from Eq. (1) for a single intracavity atom with optimum coupling  $g_0$ .

### Normal-mode splitting with large collective cooperativity

A. K. Tuchman, R. Long, G. Vrijsen, J. Boudet, J. Lee, and M. A. Kasevich

*Physics Department, Stanford University, Stanford, California 94305, USA*

(Received 3 July 2006; published 27 November 2006)

We report the observation of normal-mode splitting of the atom-cavity dressed states in both the fluorescence and transmission spectra for large atom number and observe subnatural linewidths in this regime. We also implement a method of utilizing the normal-mode splitting to observe Rabi oscillations on the <sup>87</sup>Rb ground state hyperfine clock transition. We demonstrate a large collective cooperativity,  $C = 1.2 \times 10^4$ , which, in combination with large atom number,  $N \sim 2 \times 10^5$ , offers the potential to realize an absolute phase sensitivity better than that achieved by state-of-the-art atomic fountain clocks or inertial sensors operating near the quantum projection noise limit.

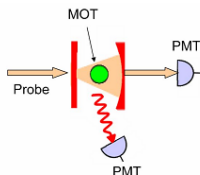


FIG. 1. (Color online) Schematic of an optical cavity shown with a MOT in the center of a hemispherical cavity mode. Probe light is incident on the planar mirror, and spectra are recorded on two PMTs: one on axis for transmission and one off axis for monitoring fluorescence.

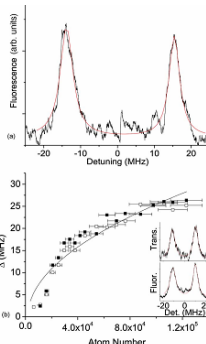


FIG. 2. (a) (Color online) The fluorescence spectrum from atoms in the cavity is shown as a function of detuning from the uncoupled atomic transition for  $N \sim 1.3 \times 10^5$ . The trace shown is

### Superradiant Rayleigh Scattering and Collective Atomic Recoil Lasing in a Ring Cavity

S. Slama, S. Bux, G. Krenz, C. Zimmermann, and Ph. W. Courteille

*Physikalisches Institut, Eberhard-Karls-Universität Tübingen, Auf der Morgenstelle 14, D-72076 Tübingen, Germany*

(Received 25 October 2006; published 1 February 2007)

Collective interaction of light with an atomic gas can give rise to superradiant instabilities. We experimentally study the sudden buildup of a reverse light field in a laser-driven high-finesse ring cavity filled with ultracold thermal or Bose-Einstein condensed atoms. While superradiant Rayleigh scattering from atomic clouds is normally observed only at very low temperatures (i.e., well below  $1 \mu\text{K}$ ), the presence of the ring cavity enhances cooperativity and allows for superradiance with thermal clouds as hot as several  $10 \mu\text{K}$ . A characterization of the superradiance at various temperatures and cooperativity parameters allows us to link it to the collective atomic recoil laser.

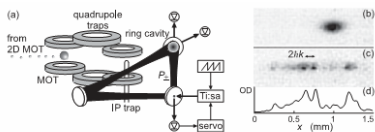


FIG. 1. (a) Schematic view of the experimental setup. A two-dimensional MOT (2D MOT) feeds a MOT in the main chamber. From here the cloud is transferred adiabatically in several intermediate steps into a Ioffe-Pritchard (IP) type magnetic trap overlapping with the ring cavity mode volume. A Ti:sapphire laser resonantly pumps the cavity mode  $P_{\pm}$ . Both cavity modes  $P_{\pm}$  are observed via the light fields leaking out through one of the cavity mirrors. The atomic cloud can be visualized by absorption imaging. Typical images of a condensate cloud at  $T = 0.5T_c$  having and not having interacted with the cavity are shown in (c) and (b), respectively. The images are recorded after 10 ms of free expansion. Curve (d) shows the vertically integrated optical density (OD) of image (c).

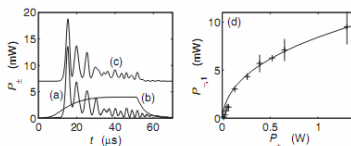
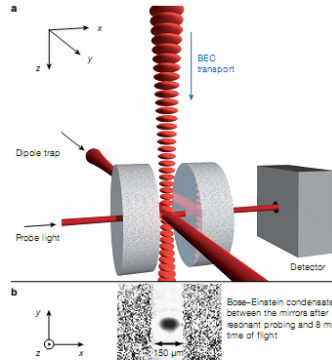


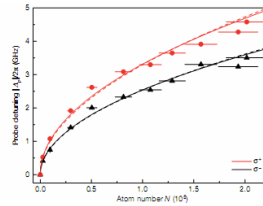
FIG. 2. (a) Measured time evolution of the reverse power  $P_{-}$ . The pump laser power is  $P_{+} = 4 \text{ W}$ . The cavity is operated at high finesse. The atom number is  $N = 1.5 \times 10^6$  and the laser wavelength is  $\lambda = 797.3 \text{ nm}$ . Curve (b) marks the time evolution of the recorded pump laser power scaled down by 1000. Curve (c) shows (offset by 7 mW) a numerical simulation of the reverse power using the above parameters (see text). To account for the finite switch-on time of the pump laser power, its experimentally recorded time evolution is plugged into the simulations, where we assume that the pump laser frequency is fixed and resonant to a cavity mode. (d) Measured and calculated (solid line) height  $P_{-1}$  of the first peak as a function of pump power  $P_{+}$ . Here  $N = 2.4 \times 10^6$  and  $\lambda = 796.1 \text{ nm}$ .

## LETTERS

## Cavity QED with a Bose–Einstein condensate

Ferdinand Brennecke<sup>1</sup>, Tobias Donner<sup>1</sup>, Stephan Ritter<sup>1</sup>, Thomas Bourdel<sup>2</sup>, Michael Köhl<sup>3</sup> & Tilman Esslinger<sup>1</sup>

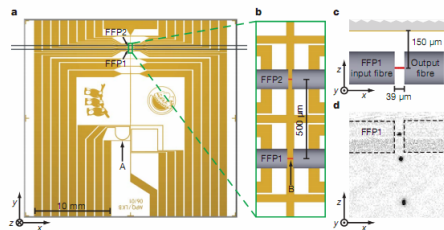
**Figure 1** Experimental situation. **a**, 36 mm above the cavity,  $3.5 \times 10^8$  ultracold atoms are loaded into the dipole potential of a vertically oriented one-dimensional optical lattice. This trumpet-shaped standing wave has its waist inside the ultrahigh-finesse cavity and is composed of two counter-propagating laser beams. A translation of the lattice transports the atoms into the cavity mode. There, they are loaded into a crossed-beam dipole trap formed by a focused beam oriented along the  $y$  axis and one of the transport beams. **b**, Almost pure condensates with  $2.2 \times 10^5$  atoms are obtained.



**Figure 4** Shift of the lower resonance of the coupled BEC-cavity system from the bare atomic resonance. The cavity was locked at  $\Delta_C = 0$ ,  $\sigma^+$  and  $\sigma^-$  polarizations are shown as red circles and black triangles, respectively. Each data point is the average of three measurements. The atom number was determined separately from absorption images with an assumed error of  $\pm 10\%$  (the vertical error bars are too small to be resolved). The dashed lines are fits of the square root dependence on the atom number, as predicted by the Lewis-Cummings model. The solid lines are fits of a more detailed theoretical model (see Methods) resulting in maximum coupling rates  $g_{\sigma^+} = 2\pi \times (1.4 \pm 0.3)$  MHz and  $g_{\sigma^-} = 2\pi \times (1.3 \pm 0.2)$  MHz. The ratio of the two coupling rates of  $1.27 \pm 0.03$  agrees with the expected ratio of 1.29 of the corresponding Clebsch–Gordan coefficients.

## LETTERS

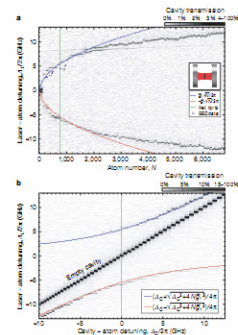
## Strong atom–field coupling for Bose–Einstein condensates in an optical cavity on a chip

Yves Colombe<sup>1\*</sup>, Tilo Steinmetz<sup>1,2\*</sup>, Guilhem Dubois<sup>1</sup>, Felix Linke<sup>1,†</sup>, David Hunger<sup>2</sup> & Jakob Reichel<sup>1</sup>

**Figure 1** Experimental set-up. **a**, Layout of the atom chip. “A” indicates the location of the first magnetic trap, loaded from a magneto-optical trap. **b**, Close-up view of the two fibre Fabry–Perot (FFP) optical cavities that are mounted on the chip. Cavity modes are drawn to scale in red. The BEC is produced in a magnetic trap and positioned in the FFP1 mode (“B”).

**c**, Geometry of the FFP1 cavity. **d**, Overlay of three CCD time-of-flight (TOF) absorption images, showing the anisotropic expansion of a BEC having interacted for 50 ms with the cavity field under conditions similar to Fig. 4. The optical fibres are outlined for clarity.

$$E_{\pm} = \hbar\omega_A + \frac{\hbar}{2} \left( \Delta_C \pm \sqrt{\Delta_C^2 + 4g_N^2} \right)$$



## Intracavity electromagnetically induced transparency

Mikhail D. Lukin, Michael Fleischhauer,\* and Marlan O. Scully

Department of Physics, Texas A&M University, College Station, Texas 77843,  
and Max-Planck-Institut für Quantenoptik, 85348 Garching, Germany

Vladimir L. Velichansky

Lebedev Institute of Physics, 53, Leninsky Prospect, Moscow, 117924 Russia

Received August 12, 1997

The effect of intracavity electromagnetically induced transparency (EIT) on the properties of optical resonators and active laser devices is discussed theoretically. Pronounced frequency pulling and cavity-linewidth narrowing are predicted. The EIT effect can be used to reduce classical and quantum-phase noise of the beat note of an optical oscillator substantially. Fundamental limits of this stabilization mechanism as well as its potential application to high-resolution spectroscopy are discussed. © 1998 Optical Society of America

The profound effects of intracavity EIT are due to large dispersion close to the point of almost-vanishing absorption,<sup>1</sup> which can easily exceed the empty-cavity dispersion in the case of an optically thick  $\lambda$  medium. To illustrate the locking and narrowing mechanism let us consider a ring cavity containing a cell of length  $l$  with a linear dispersive medium. The medium response is characterized by the real ( $\chi'$ ) and the imaginary ( $\chi''$ ) parts of the susceptibility, for which we assume  $\chi' = \beta(\nu - \nu_0)$  and constant  $\chi''$  for frequencies  $\nu$  that are sufficiently close to some resonance frequency  $\nu_0$ .  $\beta$  and  $\chi''$  are proportional to the atomic density  $N/V$ . The cavity-response function, i.e., the ratio of circulating to input intensity, is given by<sup>2</sup>

$$S(\nu) = \frac{I_{\text{circ}}}{I_{\text{in}}} = \frac{t^2}{1 + r^2 \kappa^2 - 2r\kappa \cos[\Phi(\nu)]}, \quad (1)$$

where  $t$  and  $r$  are the transmissivity and the reflectivity of the input coupler ( $t^2 + r^2 = 1$ ),  $\Phi(\nu) = \nu L/c + \kappa l \chi'/2 \approx \nu L/c + \kappa l \beta(\nu - \nu_0)/2$  is the total phase shift,

and  $\kappa = \exp(-\kappa l \chi'')$  describes the medium absorption per round trip,  $L$ . On inspection of the round-trip phase shift one finds that the resonance frequency of the combined cavity + medium system [ $\Phi(\nu_r) = 2m\pi$ ] is governed by a pulling equation:

$$\nu_r = \frac{1}{1 + \eta} \nu_c + \frac{\eta}{1 + \eta} \nu_0. \quad (2)$$

Here  $\eta = (ck/2)(l/L)\beta$  defines a frequency-locking or -stabilization coefficient and  $\nu_c$  is the resonance frequency of the empty cavity. Similarly, by expanding the cosine in Eq. (1) around  $\nu_r$ , one also finds that the width of cavity resonances  $\Delta\nu$  is changed by the intracavity medium:

$$\frac{\Delta\nu}{C} = \frac{1 - r\kappa}{\sqrt{\kappa}(1 - r)} \frac{1}{1 + \eta}, \quad (3)$$

where  $C$  is the empty-cavity linewidth.

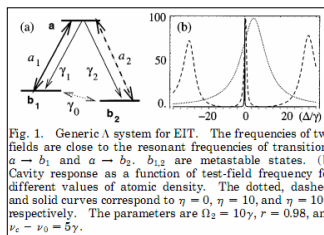


Fig. 1. Generic  $\lambda$  system for EIT. The frequencies of two fields are close to the resonant frequencies of transitions  $a \rightarrow b_1$  and  $a \rightarrow b_2$ .  $b_{1,2}$  are metastable states. (b) Cavity response as a function of test-field frequency for different values of atomic density. The dotted, dashed, and solid curves correspond to  $\eta = 0$ ,  $\eta = 10$ , and  $\eta = 100$ , respectively. The parameters are  $\Omega_2 = 10\gamma$ ,  $r = 0.98$ , and  $\nu_c - \nu_0 = 5\gamma$ .

## Vacuum Rabi splitting and intracavity dark state in a cavity-atom system

Gessler Hernandez, Jiepeng Zhang, and Yifu Zhu

Department of Physics, Florida International University, Miami, Florida 33199, USA

(Received 25 May 2007; published 12 November 2007)

We report experimental measurements of the transmission spectrum of an optical cavity coupled with cold Rb atoms. We observe the multiatom vacuum Rabi splitting of a composite cavity and atom system. When a coupling field is applied to the atoms and induces the resonant two-photon Raman transition with the cavity field in a  $\lambda$ -type system, we observe a cavity transmission spectrum with two vacuum Rabi sidebands and a central peak representing the intracavity dark state. The central peak linewidth is significantly narrowed by the dark-state resonance and its position is insensitive to the frequency change of the empty cavity.

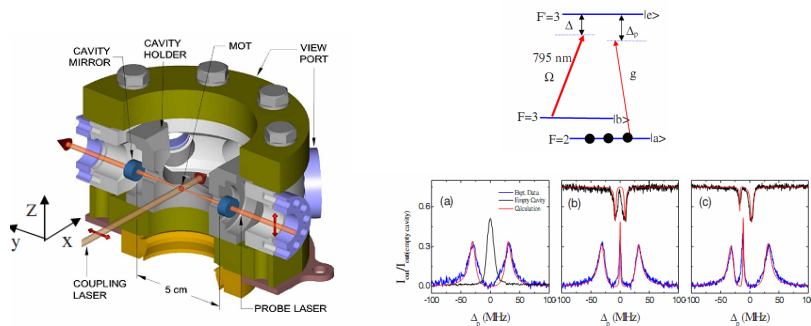


FIG. 2. (Color online) Cavity transmission versus the probe detuning  $\Delta_p$ . Blue lines are experimental data (with the background offset subtracted to fit the theoretical calculation) and red lines are the calculations. The cavity detuning  $\Delta_c = 0$ . (a)  $\Omega = 0$ . (b)  $\Omega = 8$  MHz and  $\Delta = 0$ . (c)  $\Omega = 8$  MHz and  $\Delta = -12$  MHz. For comparison, the free-space probe spectrum (in an arbitrary scale) is plotted in the top of (b) and (c), in which black (red) lines are experimental data (calculations). The other parameters used in the calculations are  $n\sigma_{1,2} = 2.5$ ,  $R = 0.97$ , and the ground state decoherence rate:  $\gamma = 0.02 \Gamma$ .

## Observation of Intracavity Electromagnetically Induced Transparency and Polariton Resonances in a Doppler-Broadened Medium

Haibin Wu, J. Gea-Banacloche, and Min Xiao

*Department of Physics, University of Arkansas, Fayetteville, Arkansas 72701, USA*  
(Received 24 September 2007; published 2 May 2008)

The transmission spectrum of three-level atoms in a vapor cell inside an optical cavity shows distinct peaks associated with atom-cavity polaritons in the system. We develop the theory of these resonances in a Doppler-broadened medium and present the results of experimental observations of these spectra in three-level  $\Lambda$ -type rubidium atoms inside an optical ring cavity.

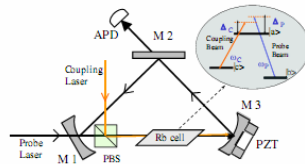


FIG. 1 (color online). Experimental setup. PBS, polarizing cubic beam splitters;  $M1$ – $M3$ , cavity mirrors; APD, avalanche photodiode detector; PZT, piezoelectric transducer.

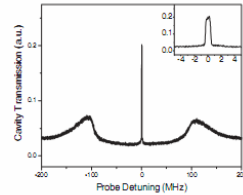


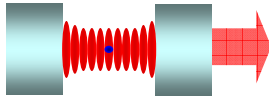
FIG. 2. The experimentally measured cavity transmission. The parameters are  $T = 67.7^\circ\text{C}$ ,  $\Omega = 120\text{ MHz}$ .

以下、チュートリアル



# パーセル因子(自然放出レートとの比)

励起された原子が、共振器の特定のモードに光子を吐くレート(Fermi's golden rule)



$$R = \frac{2\pi}{\hbar^2} |\langle g, 1 | \hbar g_0 (a\sigma^+ + a^+\sigma) | e, 0 \rangle|^2 \delta(\omega_c - \omega_A)$$

$$= 2\pi g_0^2 \frac{\kappa/\pi}{\kappa^2 + \delta^2} \xrightarrow{\omega_c = \omega_A} \frac{2g_0^2}{\kappa}$$

共振器のモード密度

$$\left( g_0 \equiv \sqrt{\frac{d_{eg}^2 \omega_c}{2\epsilon_0 \hbar V}}, \quad d_{eg} \equiv \langle e | -e\hat{x} | g \rangle, \quad 2\kappa = \frac{1}{\tau_c} = \frac{\pi c}{lF}, \quad V = \frac{\pi}{4} w_0^2 \cdot l \right)$$

共振器に吐くレートRと自然放出レート $\Gamma$ との比(パーセル因子)

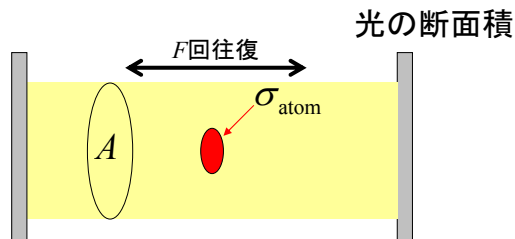
$$\frac{R}{\Gamma} = \frac{2g_0^2}{\kappa\Gamma} = 2C = \frac{3\lambda^3}{4\pi^2} \left( \frac{Q}{V} \right) \quad \left( Q \equiv \frac{\omega}{\Delta\omega} = \frac{2l}{\lambda} F \right)$$

Single-atom  
Cooperativity parameter:  $C \equiv \frac{g_0^2}{\kappa\Gamma} = \frac{12F}{\pi w_0^2 k^2} = \frac{F}{2\pi} \frac{\sigma_{\text{atom}}}{A} \quad \left( \sigma_{\text{atom}} = 6\pi\lambda^2, A = \frac{\pi}{4} w_0^2 \right)$

# Cooperativity parameterの意味

光の往復回数      散乱断面積

$$C \equiv \frac{g_0^2}{\kappa\Gamma} = \frac{12F}{\pi w_0^2 k^2} = \frac{F}{2\pi} \frac{\sigma_{\text{atom}}}{A}$$

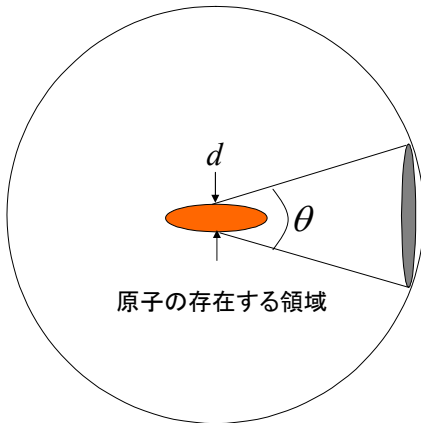


共振器内の光子が原子に吸収される確率

# Cooperatively parameterの もうひとつの意味

自由空間(F=1)の場合

$$C = \frac{\sigma_{\text{atom}}}{A} \approx \left(\frac{\lambda}{d}\right)^2$$



直径dの光源からコヒーレントに出てくる光の回折角

$$\theta \approx \frac{\lambda}{d}$$

直径dの光源からコヒーレントに出てくる光の立体角

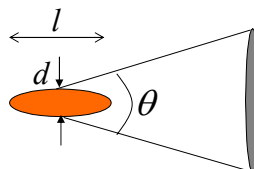
$$\Omega \approx \left(\frac{\lambda}{d}\right)^2 \approx C$$

# Cooperatively parameterの 更に別の意味(光学密度)

自由空間(F=1)かつN原子の場合

$$C \approx N \frac{\sigma_{\text{atom}}}{A} = \frac{N}{Al} \sigma_{\text{atom}} l = n \sigma_{\text{atom}} l$$

光学密度

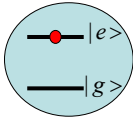


N原子の存在する領域

光学密度の高い原子集団(BEC)のCは1を超える!

# 1原子の自然放出

電気双極子演算子



$$\hat{d} = d(\sigma^+ + \sigma^-) \quad (\sigma^+ \equiv |e\rangle\langle g|, \sigma^- \equiv |g\rangle\langle e|)$$

原子と電磁場との電気双極子相互作用

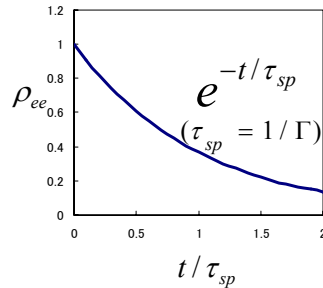
$$\hat{H}_{\text{int}} = -\hat{d} \cdot \hat{E}_{\text{rad}}$$

1原子の自然放出レート

$$R = \Gamma \langle \sigma^+ \sigma^- \rangle \quad \left( \Gamma = \frac{d^2 \omega^3}{3\pi \hbar \epsilon_0 c^3} \right)$$

励起状態の存在確率

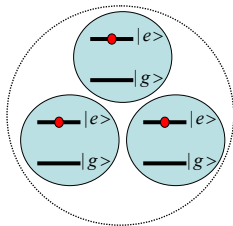
Wigner and Weisskopf (1930)



# 3原子の自然放出

原子集団の電気双極子演算子

$$\hat{d} = d \sum_{i=1}^3 (\sigma_i^+ + \sigma_i^-) \equiv d(\sigma^+ + \sigma^-)$$



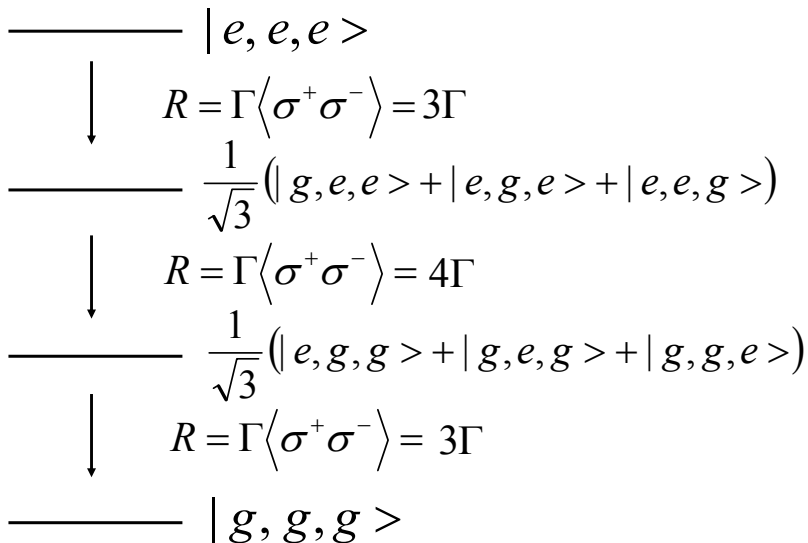
$$\left( \sigma^+ \equiv \sum_{i=1}^3 |e\rangle_{ii} \langle g|, \sigma^- \equiv \sum_{i=1}^3 |g\rangle_{ii} \langle e| \right)$$

自然放出レート

$$R = \Gamma \langle \sigma^+ \sigma^- \rangle$$

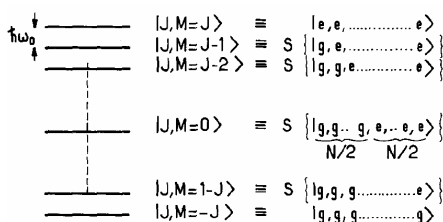
1原子の場合と同じように見えるが...

## Evolution of the three-atom system



## N原子の自然放出

N-原子系  $\Leftrightarrow$  N spin-1/2 system with the total spin  $J = N/2$   
 (必要条件: 光子の放出に関してN原子が区別がつかない)



Spontaneous emission rate of the N-atom system:

$$\begin{aligned}
 \Gamma_N &= \Gamma \langle J, M | J_+ J_- | J, M \rangle \\
 &= \Gamma (J + M)(J - M + 1) \\
 &= \Gamma N_e (N_g + 1)
 \end{aligned}$$

R. H. Dicke, Phys. Rev. **93**, 99 (1954)

↑  
 Enhancement by the number of photons already emitted

# Comparison between ordinary and superradiant emission

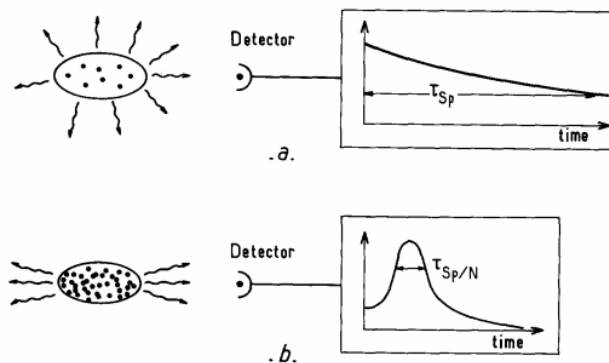


Fig. 1. Comparison between the general characteristics of ordinary fluorescence and superradiance experiments. (a) Ordinary spontaneous emission is essentially isotropic with an exponentially decaying intensity (time constant  $\tau_{sp}$ ). (b) Superradiance is anisotropic with an emission occurring in a short burst of duration  $\sim \tau_{sp}/N$ .

From M. Gross and S. Haroche, Phys. Rep. **93**, 301 (1982)